Magnetic properties of the heavy-fermion antiferromagnet CeMg₃

Pranab Kumar Das, Neeraj Kumar, R. Kulkarni, and A. Thamizhavel

Department of Condensed Matter Physics and Materials Science, Tata Institute of Fundamental Research, Homi Bhabha Road, Colaba, Mumbai 400 005, India

We have grown the single crystals of CeMg$_3$ and its nonmagnetic analog LaMg$_3$, which crystallize in the cubic crystal structure with the space group $Fm\bar{3}m$, and studied their magnetic properties on well-oriented single crystals by measuring the magnetic susceptibility, magnetization, electrical resistivity, and heat capacity. CeMg$_3$ orders antiferromagnetically with a Néel temperature T_N of 2.6 K. The specific heat capacity at low temperature exhibits an enhanced Sommerfeld coefficient of 370 mJ/K^2 mol, indicating the heavy-fermion nature of CeMg$_3$. An estimation of the Kondo temperature T_K was made and it was found that it is of a magnitude similar to that of T_N. The reduced value of the magnetization below the ordering temperature, together with the reduced entropy at the magnetic ordering temperature and the enhanced low-temperature heat capacity, indicates that Kondo effect plays a significant role in this compound. The electrical resistivity measurement suggests that CeMg$_3$ is a Kondo lattice compound. We have performed a crystalline electric field (CEF) analysis on the magnetic susceptibility and the heat capacity data and found that the ground state is a Γ_7 doublet with an overall splitting of 191 K.

I. INTRODUCTION

The magnetism due to the localized $4f$ electrons in the rare-earth-based intermetallic compounds is always interesting due to the wide range of physical properties exhibited by these compounds. The binary rare-earth intermetallic systems have been studied over several decades. In particular, the Ce-based binary compounds are the most extensively studied as they exhibit many novel magnetic behaviors owing to the close proximity of the $4f$ level to the Fermi level. For example, CeAl$_3$ and CeCu$_6$ are heavy-fermion Kondo lattice compounds without any long-range magnetic order,[1,2] and the cubic CeAl$_2$ and CeB$_6$ are Kondo lattice compounds that order magnetically at low temperature.[3,4] Pressure-induced superconductivity is observed in the binary compound CeIn$_3$.[5] In view of these interesting properties of binary compounds, we wanted to investigate the magnetic properties of RMg$_3$ (R = La and Ce) compounds which crystallize in the cubic BiF$_3$-type structure. In one of the early reports on the RMg$_3$ system, Buschow[6] has studied the magnetic properties of CeMg$_3$ and NdMg$_3$ and reported no magnetic ordering, down to 4.2 K, in these two compounds. However, Pierre *et al.*[7] and Galera *et al.*[8] have found that CeMg$_3$ orders antiferromagnetically at 3.4 K,[7,8] while NdMg$_3$ orders magnetically at 6 K.[8] From the previous neutron scattering experiments on polycrystalline samples,[9,10] it has been found that NdMg$_3$ undergoes an antiferromagnetic ordering at $T_N = 6$ K with the propagation vector $\mathbf{k}$ = (0.5, 0.5, 0.5) and the magnetic structure of NdMg$_3$ possesses ferromagnetic layers of (111) which are stacked in opposite directions leading to an antiferromagnetic alignment along the [111] axis. Recently, Tanida *et al.*[11] have performed detailed magnetic measurements on PrMg$_3$ single crystals and found that PrMg$_3$ exhibits a nonmagnetic Γ_3 doublet ground state. In this paper, we report on the detailed magnetic properties of single crystalline LaMg$_3$ and CeMg$_3$ by studying the magnetization, electrical resistivity, and heat capacity measurements. A crystal electric field (CEF) analysis was performed on the susceptibility and heat capacity data and the energy levels thus obtained corroborate the previous neutron diffraction measurements performed on polycrystalline samples.[7]

II. EXPERIMENT

From the binary phase diagram of Ce-Mg and La-Mg by Nayeb-hasehmi and Clark[12] it was found that both CeMg$_3$ and LaMg$_3$ melt congruently at a temperature close to 800 °C. Hence these compounds can be grown directly from the melt. Owing to the high vapor pressure of Mg, the single crystals were grown by the Bridgman method. The stoichiometric amounts of the rare-earth metal and magnesium were taken in a point bottomed alumina crucible and sealed in a molybdenum tube. This molybdenum tube was then subsequently sealed in a quartz ampoule and loaded into a box-type furnace. The furnace was then raised to 850 °C, well above the melting point of these compounds and held at this temperature for 24 hours. Then the samples were slowly cooled down to 780 °C over a period of 3 days. Bulk shiny single crystals were obtained by gently tapping on the alumina crucible and they were found to be stable in air. The crystals were then subjected to powder x-ray diffraction to check the phase purity. The orientation of the crystal was obtained by the back reflection Laue method. The dc magnetic susceptibility and the magnetization measurements were performed in the temperature range 1.8–300 K using a superconducting quantum interference device (SQUID) and vibrating sample magnetometer (VSM). The electrical resistivity was measured down to 1.9 K in a homemade setup. The heat capacity was measured using a Quantum Design physical property measurement system (PPMS).

III. RESULTS

A. X-ray diffraction

Small pieces of the single crystals were crushed into a fine powder and subjected to powder x-ray diffraction, using a PANalytical x-ray diffractometer with monochromatic Cu
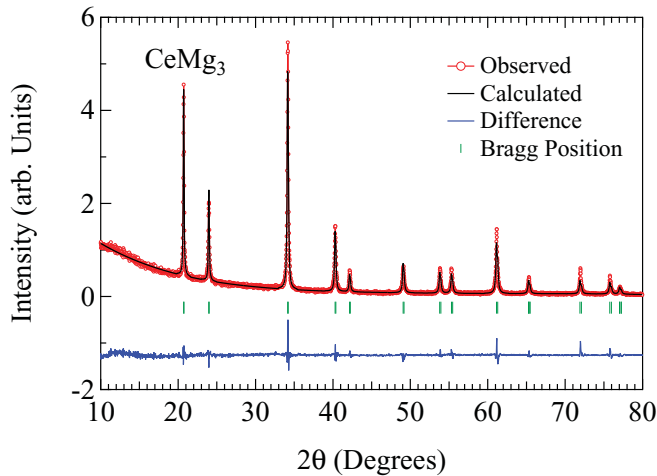
FIG. 1. (Color online) A representative powder x-ray diffraction pattern of $CeMg_3$.

K_α radiation, to check the phase purity and to estimate the lattice constant values. No traces of any secondary phases were seen in the x-ray diffractogram, indicating the samples are phase pure. A Rietveld analysis was performed and the representative powder x-ray diffraction pattern of $CeMg_3$ is shown in Fig. 1. A reasonably good fit of the experimental pattern confirms the space group $Fm\bar{3}m$ (#225) and the estimated lattice constant was 7.468 Å for $LaMg_3$ and 7.422 Å for $CeMg_3$. It is worth mentioning here that the nearest Ce-Ce distance is 5.248 Å. Hence, $CeMg_3$ is a good system to study the competing Ruderman-Kittel-Kasuya-Yosida (RKKY) interaction and Kondo screening. The stoichiometry of the samples was further confirmed by energy dispersive analysis by x-ray (EDAX) where the composition of the single crystal was analyzed at various regions of the single crystal. It was found that the sample is highly homogeneous, maintaining the stoichiometry throughout the sample. The crystals were then oriented along the principal crystallographic direction, namely, [100], by means of Laue back reflection. The fourfold symmetry of the Laue pattern confirmed the cubic structure of this compound. The crystals were then cut along [100] by means of a spark erosion cutting machine for the magnetic property measurements.

B. Magnetization

The temperature dependence of magnetic susceptibility of $CeMg_3$ from 1.8 to 300 K in an applied magnetic field of 1 kOe for H parallel to [100] direction is shown in Fig. 2(a). The inset shows the low-temperature part of the magnetic susceptibility where the susceptibility exhibits a cusp at 2.6 K and drops with the decrease in the temperature. This cusp in the magnetic susceptibility at 2.6 K is the Néel temperature of $CeMg_3$ where the Ce moments order antiferromagnetically. The magnetic ordering temperature at 2.6 K here is less than what has been reported on polycrystalline samples earlier.[8] The heat capacity measurement to be discussed later confirms the bulk magnetic ordering at this temperature. Figure 2(b) shows the inverse magnetic susceptibility. At high temperature the inverse magnetic susceptibility is linear and follows Curie-Weiss law for temperature above 200 K. The solid line in
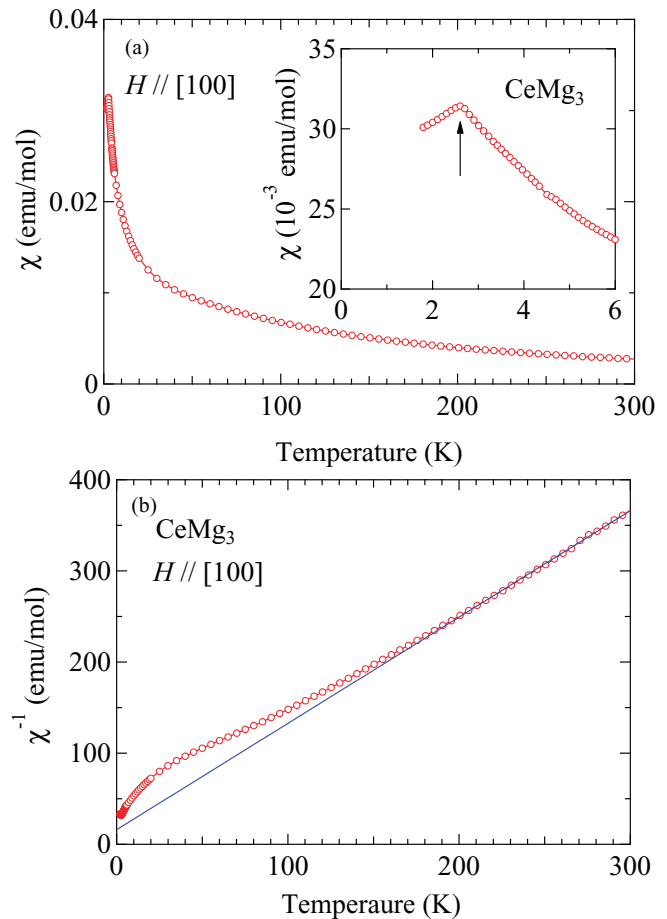

FIG. 2. (Color online) (a) Temperature dependence of magnetic susceptibility of $CeMg_3$ for field parallel to [100]. The inset shows the low-temperature part of the magnetic susceptibility in an expanded scale. (b) Inverse magnetic susceptibility of $CeMg_3$. The solid line is a fit to Curie-Weiss law.

Fig. 2(b) is a fit to the Curie-Weiss law. From the fitting, the effective magnetic moment μ_{eff} and the paramagnetic Curie temperature θ_p were found to be 2.61 μ_B/Ce and -12 K, respectively. The estimated effective moment is close to the free ion value of Ce, 2.54 μ_B in its trivalent state. The negative sign of the θ_p indicates the antiferromagnetic nature of the magnetic ordering. The inverse susceptibility deviates from the linearity for temperature less than 200 K, which is mainly attributed to the CEF effect.

The field dependence of magnetization $M(H)$ at a constant temperature $T = 1.8$ K is shown in Fig. 3. The magnetization is almost linear up to a field of 12 T, thus confirming the antiferromagnetic ordering of the Ce moments. The magnetization does not show any signature of saturation up to a field of 12 T and attains a value of only 0.5 μ_B/Ce, thus corroborating the previous neutron diffraction experimental results where an ordered moment of 0.59 μ_B is observed.[8] The saturation moment of a free Ce^{3+} ion $g_J J \mu_B$ is 2.14 μ_B with $g_J = 6/7$ and $J = 5/2$. The observed magnetization is much reduced compared to the free Ce^{3+} ion and this reduction in the magnetization is attributed to the Kondo effect and the CEF effect.
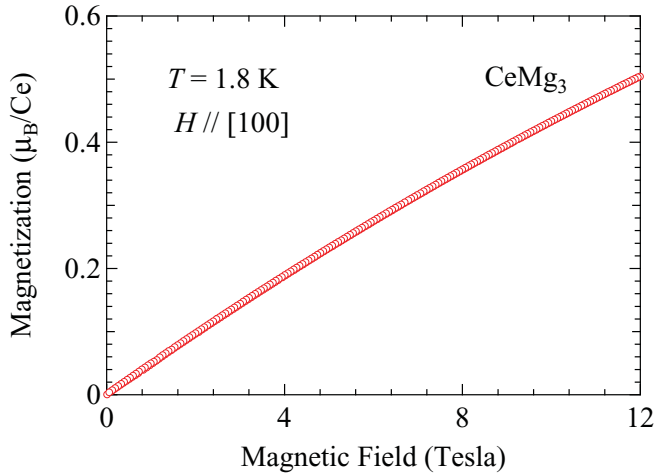
FIG. 3. (Color online) Isothermal magnetization of CeMg$_3$ for $H \parallel [100]$ at T = 1.8 K measured in a vibrating sample magnetometer.

C. Electrical resistivity

The electrical resistivity of CeMg$_3$ and LaMg$_3$ in the temperature range from 1.9 to 300 K, for current parallel to the [100] direction is shown in the main panel of Fig. 4. The antiferromagnetic ordering at 2.6 K is not clearly discernible here as the resistivity was measured down only to 1.9 K. The $\rho(T)$ of LaMg$_3$ decreases with the decrease in temperature, typical of a metallic compound without any anomaly at low temperature, while the electrical resistivity for CeMg$_3$ initially decreases with decreasing temperature and exhibits a broad curvature at around 150 K followed by a minimum at 30 K. Below 30 K, the resistivity shows a weak increase and then decreases.
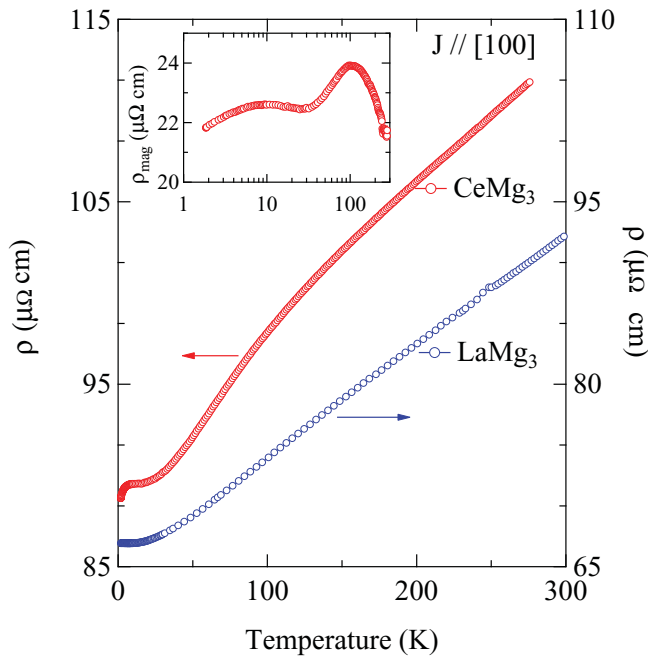

FIG. 4. (Color online) Temperature dependence of electrical resistivity $\rho(T)$ of CeMg$_3$ and LaMg$_3$ in the temperature range 1.9 to 300 K. The inset shows the magnetic part of the electrical resistivity $\rho_{mag}(T)$.

The broad hump at 150 K may be attributed to the combined influence of the crystal field and the Kondo effects. The inset shows the magnetic part of the resistivity ρ_{mag}, obtained by subtracting ρ_{LaMg_3} from ρ_{CeMg_3}, in semilogarithmic scale. ρ_{mag} increases with the decrease in temperature below 300 K and shows two broad peaks centered around 6 and 100 K. This type of double-peaked structure in $\rho_{mag}(T)$ is often observed in Kondo lattice compounds, exhibiting magnetically ordered ground states. Hence, CeMg$_3$ can be termed as a Kondo lattice compound. The $\rho_{mag}(T)$ varies nearly as $-\ln(T)$ at low and high temperatures. According to Cornut and Coqblin,[13] this type of behavior is expected for Kondo-type interaction in the presence of strong crystal field splitting with the Kondo temperature T_K much less than the overall crystal field splitting Δ_{CEF}. The low-temperature peak in $\rho_{mag}(T)$ may be attributed to the Kondo scattering of the conduction electrons with an energy scale of the order of Kondo temperature T_K. The estimation of T_K is given in Sec. IV.

D. Heat capacity

The temperature dependencies of the specific heat capacity of single crystalline CeMg$_3$ and LaMg$_3$ are shown in the main panel of Fig. 5(a). The heat capacity of LaMg$_3$ does not show any anomaly, and its temperature dependence is typical for a nonmagnetic reference compound. The low-temperature part of the heat capacity of CeMg$_3$ is shown in the top inset of Fig. 5(a), where a clear jump is seen at $T_N = 2.6$ K, confirming the bulk magnetic ordering in this compound. No anomaly is seen at 3.5 or 4 K as claimed by Galera et al.[8] in the earlier studies on polycrystalline samples. Thus the antiferromagnetic ordering in CeMg$_3$ is confirmed to be at 2.6 K. The low-temperature part of the C/T vs T^2 plot is shown in Fig. 5(a) and the magnitude of the Sommerfeld coefficient γ is obtained by fitting the expression $C/T = \gamma + \beta T^2$. The γ value thus obtained is estimated to be 370 mJ/K^2 mol, and the β value is estimated to be 608 mJ/K^4 mol. The high-temperature γ_{HT} estimated in the paramagnetic state (12 $K < T < 17 K$) results in a value of 41 mJ/K^2 mol. This implies that the enhanced low-temperature γ value is due to the strong Kondo interaction. The large value of γ in the low-temperature region indicates that CeMg$_3$ is a heavy-fermion compound, while the obtained β value implies the expected contribution from the magnons, in the magnetic structure. The large value of the γ also signals the enhanced density of the quasiparticle state at the Fermi level. The magnetic part of the heat capacity C_{mag} was estimated by the usual method of subtracting the heat capacity of LaMg$_3$ from that of CeMg$_3$. C_{mag} shows a broad peak centered around 80 K indicating the Schottky anomaly. The energy level scheme is given in Sec. IV. The C_{mag}/T versus temperature plot and the calculated entropy are shown in Fig. 5(b). At T_N (= 2.6 K) the entropy amounts to only 0.5 $R\ln 2$ with respect to the value of $R\ln 2$ anticipated for a doublet ground state. The reduced value of $R\ln 2$ further confirms the Kondo effect in CeMg$_3$.

Figure 6 shows the C/T versus T plot of CeMg$_3$ measured in applied fields of 0, 1, and 5 T. There is no appreciable change in the ordering temperature in an applied field of 1 T while in a 5-T field, the Néel temperature shifts to lower temperature and the jump in the heat capacity also decreases
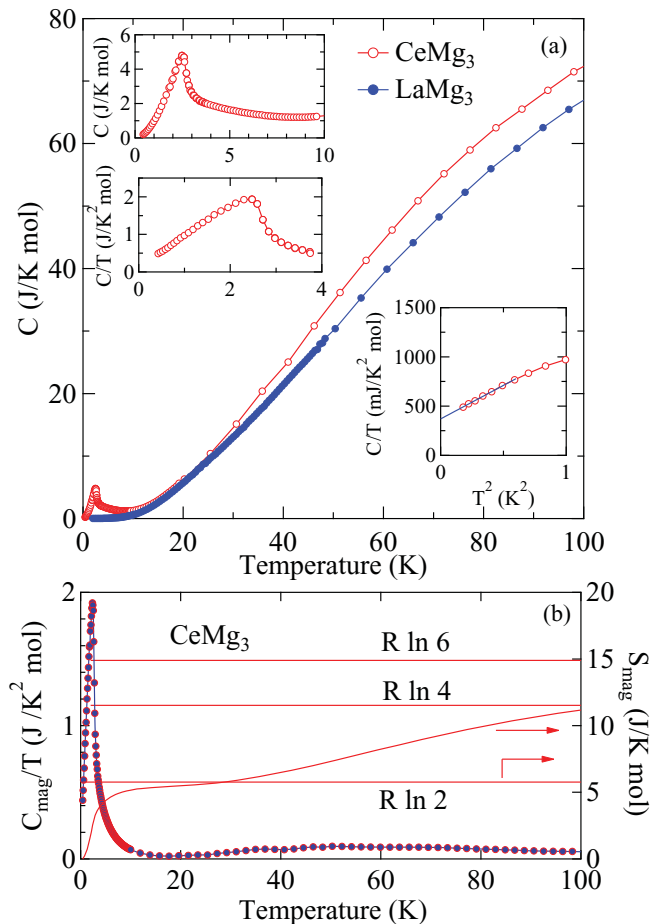
FIG. 5. (Color online) (a) Temperature dependence of the specific heat capacity in CeMg$_3$ and LaMg$_3$. The top insets show the low-temperature plots of C vs T and C/T vs T of CeMg$_3$. The bottom inset shows the C/T vs T^2 plot. (b) C_{mag}/T vs T of CeMg$_3$. The calculated entropy is plotted on the right axis.

as it is usually observed in antiferromagnetically ordering compounds. The low-temperature part of the C/T versus T^2 plot is shown in the inset of Fig. 6. An estimation of the γ value by linear extrapolation of the C/T versus T^2 plot of the heat capacity data measured in 1- and 5-T fields results in 300 and 200 mJ/K^2 mol, respectively. The reduction in the γ value implies that the application of magnetic fields tends to break the Kondo coupling between the localized $4f$ electron and the conduction electrons.

IV. DISCUSSION

The previous studies on polycrystalline samples of CeMg$_3$ have claimed that this compound orders antiferromagnetically at 4 K.[8] However, it is ubiquitous from our magnetic and thermal measurements on clean phase pure single crystals that CeMg$_3$ orders antiferromagnetically at 2.6 K. The large value of the Sommerfeld coefficient γ at low temperature indicates enhanced density of states at the Fermi level which is due to the result of the Kondo effect. The electrical resistivity measurement clearly indicates that CeMg$_3$ is a Kondo lattice compound. The reduced value of the magnetic moment of 0.5 μ_B/Ce at $T = 1.8$ K in a field of 12 T and a very small heat
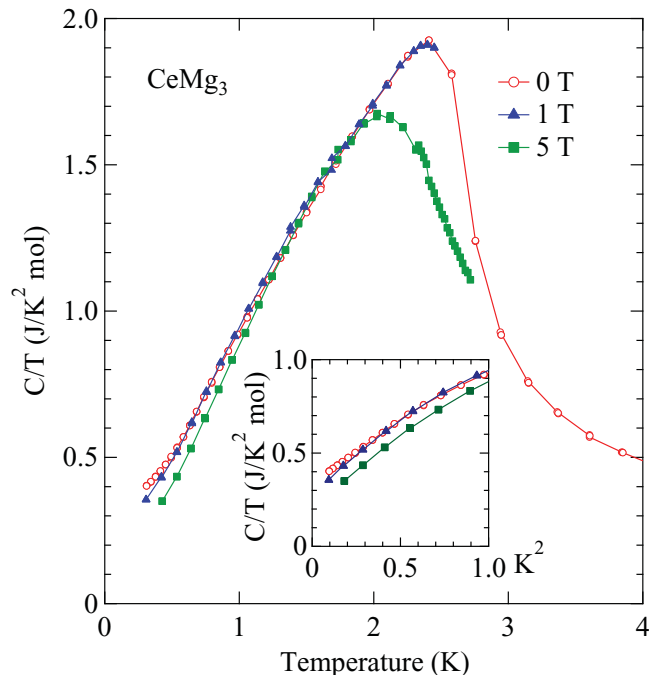

FIG. 6. (Color online) (a) C/T versus T plot of CeMg$_3$ in applied magnetic fields, in the temperature range 0.5 to 4 K. The inset shows the low-temperature part of the C/T versus T^2 plot.

capacity jump at the magnetic ordering temperature further confirm the Kondo effect in CeMg$_3$. We made an estimate of the Kondo temperature T_K by the method described by Bredl *et al.*,[14] where in the mean field approach, the jump in the heat capacity ΔC_{mag} of a Kondo system is related to the Kondo temperature. Besnus *et al.*[15] have found that the estimation of T_K by this model agrees well with the experimental data on various Ce and Yb compounds. From Eqs. (12), (13), and (15) of Ref. 14, Blanco *et al.*[16] have given the expression for ΔC_{mag} at the magnetic ordering temperature as

$$\Delta C_{mag} = \frac{6N_A k_B}{\psi'''\left(\frac{1}{2}+x\right)}\left[\psi'\left(\frac{1}{2}+x\right)+x\psi''\left(\frac{1}{2}+x\right)\right]^2,$$
(1)

where $x = (T_K/T_N)/2\pi$ and ψ', ψ'', and ψ''' are the first, second, and third derivative of the polygamma function and the other terms have the usual meaning. A plot of this function is shown in Fig. 7. The jump in the magnetic part of the heat capacity was estimated to be 4.35 J/K mol, which results in a T_K value of 3.5 K. Desgranges and Schotte[17] have theoretically explained that the entropy of a Kondo system at the characteristic temperature T_K amounts to 0.68 $R \ln 2$ (= 3.92 J/K mol). According to this expression, for CeMg$_3$, 0.68 $R \ln 2$ is reached at 3.8 K, which indicates that this Kondo temperature is in close agreement with the one estimated from Eq. (1). Furthermore, the Kondo temperature can also be estimated from the paramagnetic Curie-Weiss temperature as mentioned by Grüner and Zawadowski,[18] $|\theta_p|/4(12/4 = 3$ K). The estimation of the Kondo temperature T_K by various methods gives a value of 3–4 K, which is close to the magnetic ordering temperature of CeMg$_3$. However, a detailed neutron

diffraction experiment has to be performed to substantiate our estimation of T_K.

The magnetic part of the heat capacity C_{mag} of CeMg$_3$ shows a broad peak at high temperature as shown in Fig. 8(a). This feature is attributed to the Schottky excitations between

$$C_{Sch}(T) = R \left[\frac{\sum_i g_i e^{-E_i/T} \sum_i g_i E_i^2 e^{-E_i/T} - \left[\sum_i g_i E_i e^{-E_i/T} \right]^2}{T^2 \left[\sum_i g_i e^{-E_i/T} \right]^2} \right], \quad (2)$$

where R is the gas constant, E_i is the CEF energy level in units of temperature and g_i is the corresponding degeneracy. The Ce atom in CeMg$_3$ possesses a cubic site symmetry and hence the ground state should be a doublet or quartet. From the entropy calculations discussed above, it is obvious that the ground state of CeMg$_3$ should be a doublet ground state. Considering a degeneracy of doublet ground state and a quartet excited state, we found that the CEF levels are separated by an energy of 191 K apart. The solid line in Fig. 8(a) indicates the calculated Schottky heat capacity which is matching well with the experimental data.

The crystalline electric field analysis was also performed on the magnetic susceptibility data. For a cubic point symmetry, the CEF Hamiltonian is given by

$$\mathcal{H}_{CEF} = B_4^0 \left(O_4^0 + 5O_4^4 \right) + B_6^0 \left(O_6^0 - 21O_6^4 \right), \quad (3)$$

where B_l^m and O_l^m are the crystal field parameters and the Steven's operators, respectively.[19,20] For the Ce atom, the sixth-order terms O_6^0 and O_6^4 vanish and hence the CEF Hamiltonian reduces to

$$\mathcal{H}_{CEF} = B_4^0 \left(O_4^0 + 5O_4^4 \right). \quad (4)$$

the CEF levels of the Ce^{3+} ions. We have performed an analysis of the heat capacity and the magnetic susceptibility data on the basis of the CEF model. The Schottky contribution to heat capacity is given by the following expression,

The CEF susceptibility is given by the following expression,

$$\chi_{CEFi} = N(g_J \mu_B)^2 \frac{1}{Z} \left(\sum_{m \neq n} |\langle m| J_i |n\rangle|^2 \frac{1 - e^{-\beta \Delta_{m,n}}}{\Delta_{m,n}} e^{-\beta E_n} \right.$$

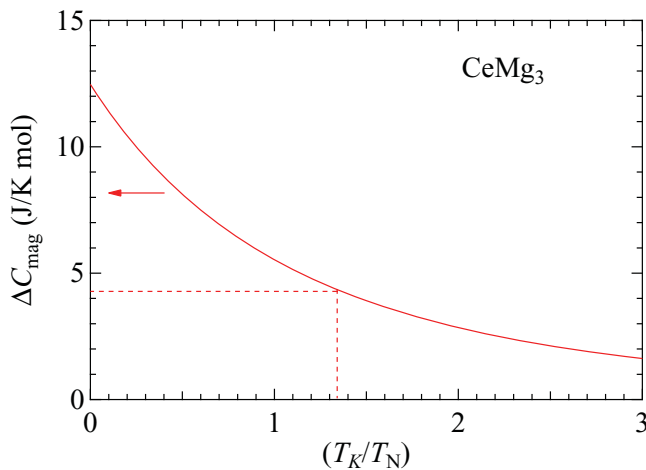$$\left. + \sum_n |\langle n|J_i |n\rangle|^2 \beta e^{-\beta E_n} \right), \quad (5)$$

FIG. 7. (Color online) Estimation of the Kondo temperature from the jump in the magnetic part of the heat capacity. The solid line is the plot of Eq. (1). See text for details.
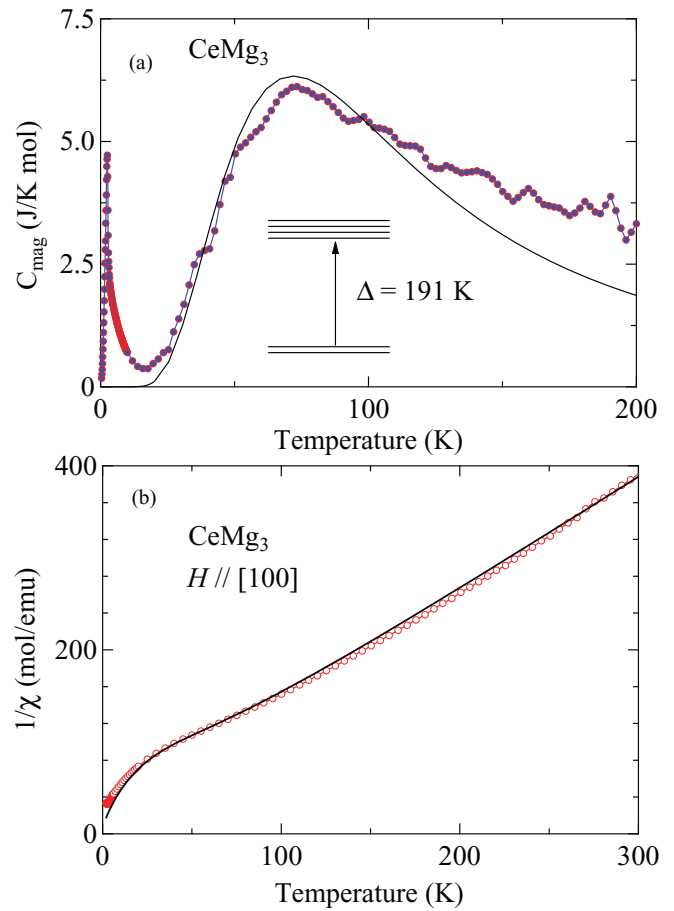

FIG. 8. (Color online) (a) Magnetic part of the specific heat capacity of CeMg$_3$. The solid line is the calculated Schottky heat capacity, which gives an energy separation of 191 K between the ground state doublet and the excited quartet. (b) Inverse magnetic susceptibility of CeMg$_3$. The solid line is based on the CEF calculation.

where g_J is the Landé g factor, and E_n and $|n\rangle$ are the nth eigenvalue and eigenfunction, respectively. J_i ($i = x$, y, and z) is a component of the angular momentum, $\Delta_{m,n} = E_n - E_m$, $Z = \sum_n e^{-\beta E_n}$, and $\beta = 1/k_{\rm B}T$. The magnetic susceptibility including the molecular field contribution λ_i is given by

$$\chi_i^{-1} = \chi_{{\rm CEF}i}^{-1} - \lambda_i. \qquad (6)$$

The CEF parameter B_4^0 was estimated by using Eqs. (4)–(6). The solid line in Fig. 8(b) is the calculated CEF curve and the value of B_4^0 thus obtained is 0.53 K and the molecular field contribution λ is -8 mol/emu. The sign of the B_4^0 parameter is positive, which clearly indicates that the ground state is a Γ_7 doublet. From the eigen values of the crystal field Hamiltonian the crystal field splitting energy was found to be 191 K. The crystal field level scheme thus obtained from the magnetic susceptibility and the heat capacity data are in accordance with the previous neutron diffraction results on polycrystalline samples.[7,9] The magnitude of the ordered moment of a Γ_7 doublet ground state based on the CEF calculation ($g_J J_x = 6/7 \times 0.833$) should be 0.714 $\mu_{\rm B}$/Ce. The observed magnetization value at 1.8 K is only 0.56 $\mu_{\rm B}$/Ce, this confirms that the moment reduction in this compound is due to the combined effect of Kondo and crystal field effects.

The overall magnetic behavior of CeMg$_3$ resembles to that of the popular antiferromagnetically ordered heavy-fermion systems like CeIn$_3$,[21] CePd$_2$Si$_2$,[5] and CeCu$_2$Ge$_2$.[22] These systems have their Néel and Kondo temperatures nearly equal and exhibit pressure-induced superconductivity. The ordered moments in these compounds are also considerably reduced, and these compounds also possess an enhanced Sommerfeld coefficient γ, as it has been observed in the present CeMg$_3$

system. All these imply that CeMg$_3$ is another compound where the high-pressure studies will yield some interesting results.

V. CONCLUSION

Single crystals of LaMg$_3$ and CeMg$_3$ were grown by the Bridgman method in sealed molybdenum tubes. X-ray and EDAX analysis of the sample confirmed the stoichiometry of the single crystals. The magnetic susceptibility and the heat capacity clearly indicated the antiferromagnetic ordering at $T_{\rm N} = 2.6$ K.

The heavy-fermion nature of this compound is confirmed by the large Sommerfield coefficient $\gamma = 370$ mJ/K^2 mol. The reduced value of the magnetization, the reduced magnetic entropy at the magnetic ordering temperature, and the $-\ln(T)$ behavior in the electrical resistivity confirmed the significant contribution of the Kondo effect in CeMg$_3$. The estimated Kondo temperature $T_{\rm K}$ was found to be 3–4 K which is close to the magnetic ordering temperature, suggesting a delicate competition between the Kondo effect and the indirect exchange interaction. Since $T_{\rm N}$ and $T_{\rm K}$ are very close in CeMg$_3$, it will be interesting to study the effect of pressure on the electrical resistivity of CeMg$_3$, which is planned for the future. The CEF analysis of the heat capacity and the magnetic susceptibility data indicated that the ground state is a Γ_7 doublet while the excited state is a Γ_8 quartet with an energy splitting of 191 K.

[1]K. Andres, J. E. Graebner, and H. R. Ott, Phys. Rev. Lett. **35**, 1779 (1975).

[2]Y. Ōnuki, Y. Shimizu, and T. Komatsubara, J. Phys. Soc. Jpn. **53**, 1210 (1984).

[3]B. Barbara, J. X. Boucherle, J. L. Buevoz, M. F. Rossignol and J. Schweizer, Solid State Communications **24**, 481 (1977).

[4]K. Winzer, Solid State Commun. **16**, 521 (1975).

[5]F. M. Grosche, I. R. Walker, S. R. Julian, N. D. Mathur, D. M. Freye, M. J. Steiner, and G. G. Lonzarich, J. Phys. Condens. Matter **13**, 2845 (2001).

[6]K. H. J. Buschow, J. Less-Common Met. **44**, 301 (1976).

[7]J. Pierre, A. P. Murani, and R. M. Galera, J. Phys. F: Met. Phys. **11**, 679 (1981).

[8]R. M. Galera, J. Pierre, and J. Pannetier, J. Phys. F: Met. Phys. **12**, 993 (1982).

[9]R. M. Galera, A. P. Murani, and J. Pierre, J. Magn. Magn. Mater. **23**, 317 (1981).

[10]T. Chatterji, G. J. Schneider, and R. M. Galera, Phys. Rev. B **78**, 012411 (2008).

[11]H. Tanida, H. S. Suzuki, S. Takagi, H. Onodera, and K. Tanigaki, J. Phys. Soc. Jpn. **75**, 073705 (2006).

[12]B. Nayeb-hashemi and J. Clark, Bull. Alloy Phase Diagrams **9**, 916 (1988).

[13]B. Cornut and B. Coqblin, Phys. Rev. B **5**, 4541 (1972).

[14]C. D. Bredl, F. Stglich, and K. D. Schotte, Z. Phys. B **29**, 327 (1978).

[15]M. J. Besnus, A. Braghta, N. Hamdaoui, and A. Meyer, J. Magn. Magn. Mater. **104-107**, 1385 (1992).

[16]J. A. Blanco, M. de Podesta, J. I. Espeso, J. C. Gómez Sal, C. Lester, K. A. McEwen, N. Patrikios, and J. Rodríguez Fernández, Phys. Rev. B **49**, 15126 (1994).

[17]H.-U. Desgranges and K. D. Schotte, Phys. Lett. A **91**, 240 (1982).

[18]G. Grüner and A. Zawadowski, Rep. Prog. Phys. **37**, 1497 (1974).

[19]K. W. H. Stevens, Proc. Phys. Soc. London, Sect. A **65**, 209 (1952).

[20]M. T. Hutchings, in *Solid State Physics: Advances in Research and Applications*, edited by F. Seitz and B. Turnbull (Academic Press, New York, 1965), Vol. 16, p. 227.

[21]G. Knebel, D. Braithwaite, P. C. Canfield, G. Lapertot, and J. Flouquet, Phys. Rev. B **65**, 024425 (2001).

[22]D. Jaccard, K. Behnia, and J. Sierro, Phys. Lett. A **163**, 475 (1992).